J Mater Sci (2006) 41:6328–6332
DOI 10.1007/s10853-006-0501-1

Tensile behavior and deformation mechanisms of bulk ultrafine-grained copper

S. J. Xie · P. K. Liaw · H. Choo

Received: 14 July 2004 / Accepted: 18 August 2005 / Published online: 24 August 2006

Abstract The tensile behaviors of the ultrafine-grained (UFG) pure copper prepared by cold rolling have been investigated. The UFG-Cu exhibited high strengths and low ductility. The ductile dimple-like fracture surfaces and persistent-slip-bands (PSBs)-like local shear bands in the tension-deformed UFG-Cu were observed, both of which typically spanned tens of grain sizes. This observation indicated that the fracture mechanisms operated at a larger scale than the grain size and eventually involved collective grain activities. Moreover, localized shear bands provided the experimental evidence to the localized plastic deformation, which was the one of the dominant reasons, causing the low ductility in the UFG-Cu.

Introduction

Nanocrystalline (nc) and sub-microcrystalline (ultrafine-grained, UFG) metals and alloys have attracted much attention in recent years [1–10], due to their ultra-high yield and fracture strengths, superior wear resistances in comparison to conventional microcrystalline materials. It was reported that nc copper produced by the surface-mechanical attrition treatment (SMAT) exhibited a yield strength as high as 760 MPa [1]; the Al-1.71 atomic percent (at.%) Fe alloy produced by the electron-beam deposition showed an abnormally high tensile strength of approximately 950 MPa [2]; and the yield strength of the nc vanadium, prepared by the high-energy ball milling and followed by the consolidation, reached 2.0 GPa [3]. However, the literature survey also showed that most of nc/UFG metals and alloys exhibited relatively poor ductility, and their ductility decreased with decreasing grain sizes, which limited their applications [11].

It is now generally accepted that the limited uniform deformation results from the restricted dislocation activities in the nanosized/ultrafine grains and localized deformation [12–14]. A dominant surface feature of the localized deformation is the appearance of shear bands. Shear bands in the compressively deformed nanostructured Fe were reported by Wei et al. [15]. The persistence of shear bands as persistent slip bands in the cyclically-deformed UFG copper was observed by Agnew and Weertman [16], and verified by other investigators [17–19]. However, in the tensile test of nc/UFG metals, the local shear bands are very difficult to be observed and so little reported. In this paper, the local shear bands in the tensile-deformed UFG-Cu, whose morphologies are similar to those of persistent-slip-bands (PSBs)-like local shear bands in the cyclically deformed UFG-Cu, are reported, and, then, its deformation and damage-evolution mechanisms are explored, based on the microstructural examination of the fracture surfaces and side faces of the fractured UFG-Cu.

Experimental procedure

The UFG copper sample was synthesized by rolling a pure commercial Cu (99.99%) bar 20 passes to 900% deformation, with the liquid-nitrogen-temperature

S. J. Xie · P. K. Liaw (✉) · H. Choo
Department of Materials Science & Engineering,
The University of Tennessee, Knoxville, TN 37996, USA
e-mail: pliaw@utk.edu

(LNT) cooling of the samples between consecutive rolling passes [4]. The degree of deformation was defined by $\varepsilon = (\delta_0 - \delta)/\delta$, where δ_0 (= 10 mm) and δ (= 1 mm) are the initial and final thicknesses of samples, respectively.

The microstructure of the cold-rolled copper was characterized by means of the X-ray diffraction (XRD) analyses and transmission-electron-microscopy (TEM) observations. Quantitative X-ray diffraction measurements of the UFG copper were carried out in a Philips X'pert X-Ray Diffractometer with the Copper Kα radiation at 40 kV and 30 mA. The average grain size was determined in terms of the diffraction-line broadening of the five single Bragg reflection peaks: (111), (200), (220), (311), and (222), according to the Scherrer equation and Williamson–Hall method [20], while correcting for the instrumental-line broadening, using the standard Si sample.

The TEM experiments were performed on the H-800 transmission-electron microscope at an operating voltage of 100 KV. The TEM samples were prepared by the conventional electrochemical-polishing technique. First, the samples, 3 mm in diameter, were punched from the cold-rolled copper plate. These samples were ground to about 100 μm in thickness, using sandpapers ranging from 200 to 800 grit, and, then, the samples were thinned by electrochemical polishing, using a 25 volume percent (vol.%) H_3PO_4 + 25 vol.% C_2H_5OH + 50 vol.% H_2O solution at 22 V. TEM images are quantified in two methods. In the first method, the well-defined, large-angle grain boundaries are drawn into a contour map. The Heyn Linear Intercept Procedure according to the American Society for Testing and Materials (ASTM) Standard [21] is used to produce the bar graph of the size distribution and mean grain size. In the second method, typical grains in a good contrast orientation are selected and finer contour maps are produced. These contour maps were also quantified by the same Linear Intercept method to obtain the average subgrain size. The grain-size distribution is expressed by the grain size versus the relative number of grains, which is defined by the number of grains in a size range, divided by the maximum number of grains, in the all size range.

For the mechanical-property measurements, all the samples were cut and polished to a width of 2 mm, a thickness of 0.8 mm, and a gauge length of 9.525 mm. Note that the previously reported tensile tests of nanostructured metals typically used a gauge length in the range of 1–5 mm. Uniaxial tensile tests were done under a constant nominal strain rate of 1×10^{-4} s^{-1} using the Material Test System (MTS) Model 810 load frame at room temperature. Following the material testing, the fracture surfaces and side faces were carefully examined, using a scanning-electron microscope (SEM) and optical microscope, respectively.

Results and discussions

Microstructures

Figure 1(a) is the metallograph of the as-received coarse-grained (CG) copper, whose grain sizes are in the range of 100–200 μm. The typical TEM bright-field image and selected-area-diffraction (SAD) pattern of the as-rolled copper are shown in Fig. 1(b) and (c), respectively. From Fig. 1(b), we can see that grains are ultrafine and somewhat inhomogeneous, as indicated

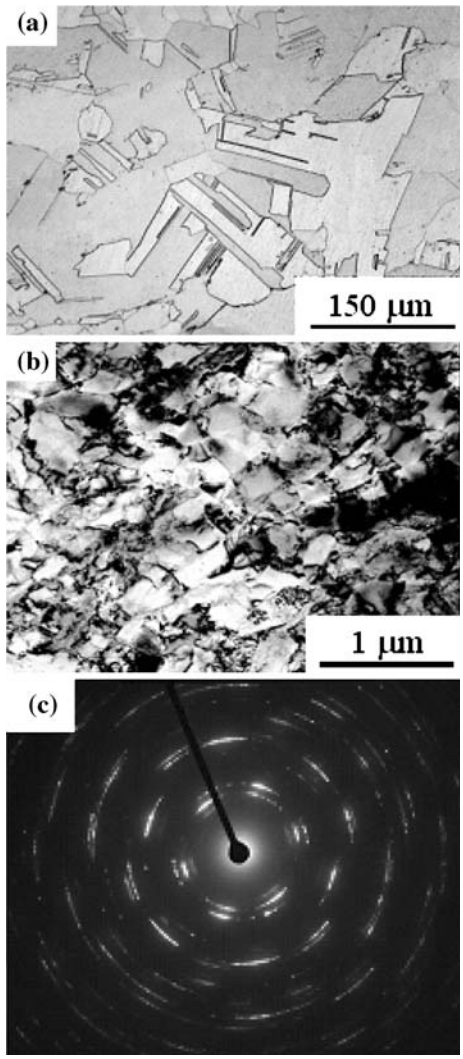

Fig. 1 (**a**) Metallograph of the as-received CG-Cu, (**b**) TEM bright-field image of the as-rolled UFG-Cu, (**c**) Selected-Area-Diffraction (SAD) pattern corresponding to Figure 1 (**b**)

by the SAD pattern presented in Fig. 1(c) with non-uniform and discontinuous rings, which suggest that the majority of the angles between grain boundaries are fairly low. All diffraction rings in the SAD pattern were identified as the face-centered-cubic (fcc) Cu, and no other phases were detected.

The grain-size distributions obtained from the large-angle grain boundaries contour in TEM images and from XRD method were shown in Fig. 2, which shows that the grain size (164 nm) obtained by large-angle grain boundaries and size distribution are much larger than that obtained by the X-ray method. The average size (91 nm), obtained from the finer contours corresponds to subgrains or dislocation cells, is close to that (86 nm) determined from x-rays. This trend indicates that in a bulk specimen, the crystallite size obtained by the X-ray method is closer to the subgrain or dislocation-cell size. It is noted that the later-mentioned TEM grain size means the value obtained from the large-angle grain boundaries contour in TEM images.

Tensile behavior

Figure 3 shows a tensile engineering stress-strain curve for the cold-rolled UFG-Cu in comparison with that for the as-received CG-Cu, obtained under uniaxial tension at a strain rate of 1×10^{-4} s^{-1}. The cold-rolled UFG-Cu exhibits little uniform deformation with a nearly perfect plastic behavior when strains are above 12%, while the CG-Cu shows a large uniform deformation up to a 46% strain. A uniform deformation appears to decrease with decreasing grain sizes and is largely inhibited in the heavily cold-rolled copper. The limited uniform deformation in the UFG-Cu may be attributed to the limited dislocation activity in the ultrafine grains. For coarse-grained polycrystals, the plastic deformation is carried by dislocations, which are continuously nucleated at sources within the grains. In the ultrafine crystalline regime, the spatial confinement of the much smaller grains inhibits the operation of dislocation sources inside grains, limiting the dislocation activity and, therefore, the uniform plastic deformation [23].

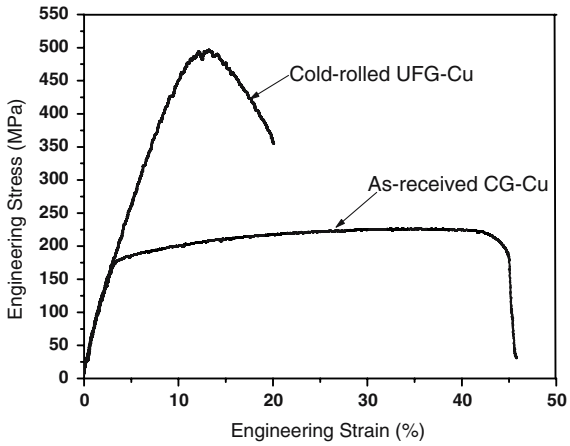

Fig. 3 Tensile engineering stress-strain curves for the as-received CG-Cu and cold-rolled UFG-Cu at a strain rate of 1×10^{-4} s^{-1}

Deformation mechanism

The scanning-electron micrograph of the fracture surface of the UFG-Cu made by cold rolling is shown in Fig. 4. The image indicates that the local failure process is ductile in the UFG-Cu, with the mechanism of failures arising from the nucleation, growth, and linkup of voids. The dimple sizes on the fracture surface in UFG metals are in the range of 2–6 μm. However, the mean grain size is 164 nm for this material, which resulted from a TEM grain-size distribution analysis.

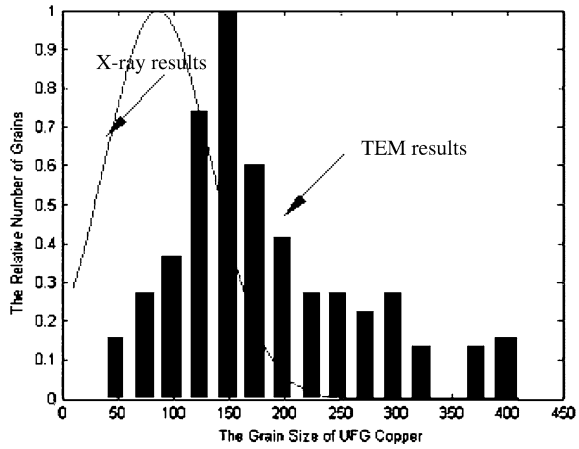

Fig. 2 Grain-size distribution obtained by the TEM images and the XRD method

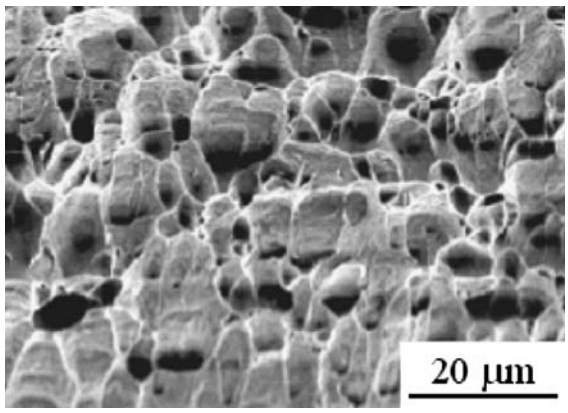

Fig. 4 Scanning-electron microscopy of typical dimple-like features on the fracture surface of the UFG-Cu

This observation suggests that fracture mechanisms may operate at a larger scale than the grain size and eventually involve the collective activity of tens of grains. Similar dimple-like features with an average dimple size of several or tens of grain sizes have also been observed in electrodeposited nanocrystalline metals [24, 25] and cold-rolled UFG Ti [26].

The view of the side flat faces of the tensile-fractured UFG-Cu is shown in Fig. 5. The shear markings (some indicated by white arrows), oriented 55–65° away from the tensile axis, may be called persistent-slip-bands (PSBs)-like shear bands only because their morphologies are similar to those of PSBs in coarse-grained metals after fatigue tests [27]. It should be noted that PSBs-like shear bands formed in cyclic deformation might be attributed to both oriented distributions of defects along shear planes and reversible cyclic deformation [19], which is not the case of PSBs-like shear bands formed in tensile deformation. The PSBs-like shear bands formed in tensile deformation generally appear in groups and are approximately parallel to one another. The spacing between shear bands is in the range of 2–6 μm, and the lengths of shear bands are tens of micrometers. Since the grain size of the sample is about 164 nm, there are at least tens of ultrafine grains between shear bands, which also indicates that the localized plastic deformation represented by shear bands may operate at a larger scale than the grain size and eventually involve the collective grain activity.

The importance of local shear planes in the deformation mechanism of nanocrystalline metals has been proposed in the model of Hahn and Padmanabhan [28]. According to the model, local shear planes were concentrated around their neighbouring planes, creating a cluster of grains embedded in a sliding environment because of the presence of grain boundaries (GBs) that are resistant to sliding, such as low-angle GBs and twins. Thus, a plasticity-length scale, corresponding to the dimensions of the dimple structures and the spacing distances between local shear bands observed in the tensile-deformed surface, emerges on the order of several or tens of grain sizes. Our experimental results are consistent with the simulations and provide the experimental evidence that dimples on ultrafine/nano crystalline fracture surfaces can be evidenced for the shear-plane formation [23].

Moreover, the localized shear deformation in the UFG-Cu can lead to early failures, especially in tension where spatial confinements are absent. And the intrinsic material ductility will be limited in UFG metals because their dislocation generation and movement are largely inhibited. Therefore, the fracture is expected at little deformation and concentrated in severely localized deformation bands.

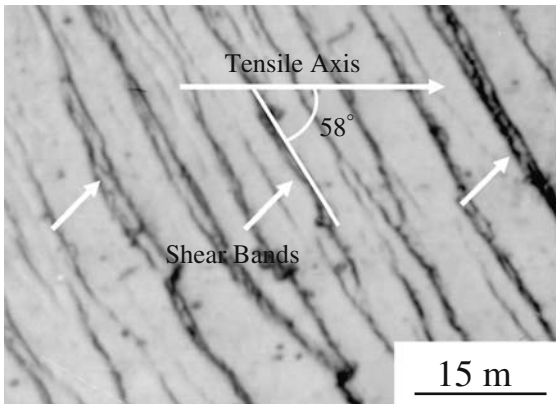

Fig. 5 Side flat face of a tensile sample after fracture, showing a number of shear markings oriented 55–65° away from the tensile axis

Summary and conclusions

The tensile behaviors of the UFG-Cu in comparison with the CG-Cu have been characterized. The observation of fracture surfaces and side flat faces in tension-deformed samples showed that the UFG-Cu is ductile during the tensile fracture. However, ultrafine grains inhibited the dislocation activities. Thus, the PSB-like local shear bands appeared, the UFG-Cu exhibited low ductilities, and its fracture mechanisms operated at a larger scale than the grain size and eventually involved the collective grain activity.

Acknowledgement The present work was supported by the NSF International Materials Institutes (IMI) Program, under DMR-0231320, with Dr. Carmen Huber as the Program Director.

References

1. Wang YM, Wang K, Pan D, Lu K, Hemker KJ, Ma E (2003) Scripta Mater 48:1581
2. Mukai T, Suresh S, Kita K, Sasaki H, Kobayashi N, Higashi K, Inoue A (2003) Acta Mater 51:4197
3. Wei Q, Jiao T, Ramesh KT, Ma E (2004) Scripta Mater 50:359
4. Wang YM, Chen MW, Zhou FH, Ma E (2003) Nature 419:912
5. Fan GJ, Fu LF, Qiao DC, Choo H, Liaw PK, Browning ND (2006) Scripta Mater 54(12):2137
6. Fan GJ, Wang YD, Fu LF, Choo H, Liaw PK, Ren Y, Browning ND (2006) Appl Phys Lett 88(17): Art. No. 171914
7. Fan GJ, Choo H, Liaw PK, Lavernia EJ (2006) Acta Mater 54(7):1759
8. Fan GJ, Choo H, Liaw PK, Lavernia EJ (2005a) Mat Sci Eng A-Struct 409(1–2):243

9. Fan GJ, Choo H, Liaw PK, Lavernia EJ (2005b) Metall Mater Trans A 36A(10):2641
10. Fan GJ, Wang GY, Choo H, Liaw PK, Park YS, Han BQ, Lavernia EJ (2005) Scripta Mater 52(9):929
11. Koch CC, Morris DG, Lu K, Inoue A (1999) MRS Bull 24:54
12. Weertman JR (2002) Mater Sci Forum 386-3:519
13. Schiotz J, Di Tolla FD, Jacobson KW (1998) Nature 391:561
14. Van Swygenhoven H (2002) Science 296:66
15. Wei Q, Jia D, Ramesh KT, Ma E (2002) Appl Phys Lett 81:1240
16. Agnew SR, Weertman JR (1998) Mater Sci Eng A244:145
17. Wu SD, Wang ZG, Jiang CB, Li GY, Alexandrov IV, Valiev RZ (2003) Scripta Mater 48:1605
18. Hashimoto S, Kaneko Y, Kitagawa K, Vinogradov A Yu, Valiev RZ (1999) Mater Sci Forum 312–314:593
19. Vinogradov AY, Patlan V, Hashimoto S, Kitagawa K (2002) Phil Mag A82:317
20. Williamson GK, Hall WH (1953) Acta Metall 1:22
21. Annual Books of ASTM Standards (2001) 3:251
22. Ungár T (2003) Adv Eng Mater 5:323
23. Hasnaoui A, Swygenhoven HV, Derlet PM (2003) Science 300:1550
24. Wang YM, Ma E, Chen MW (2002) Appl Phys Lett 80:2395
25. Kumar KS, Suresh S, Chisholm MF, Horton JA, Wang P (2003) Acta Mater 51:387
26. Jia D, Wang YM, Ramesh KT, Ma E, Zhu YT, Valiev RZ (2001) Appl Phys Lett 79:611
27. Basinski ZS, Basinksi SJ (1985) Acta Metall 33:1307
28. Hahn H, Padmanabhan KA (1997) Philos Mag B76:559